RSC Advances

Cite this: *RSC Advances*, 2012, **2**, 12148–12152

www.rsc.org/advances

COMMUNICATION

Using a polyhedral oligomeric silsesquioxane surfactant and click chemistry to exfoliate montmorillonite†

Hui-Wang Cui and Shiao-Wei Kuo*

Received 24th August 2012, Accepted 17th October 2012
DOI: 10.1039/c2ra21917d

In this study, we prepared exfoliated montmorillonite (MMT) through Huisgen [2 + 3] cycloadditions (click reactions) of a propargyl-containing intercalator with singly or multiply azido-functionalized polyhedral oligomeric silsesquioxane nanoparticles. Wide-angle X-ray diffraction, Fourier transform infrared spectroscopy, transmission electron microscopy, and thermogravimetric analyses revealed the structures and properties of the products, which have the potential to be used directly through simple polymer blending or copolymerization to improve the physical properties of polymer-based clay nanocomposites.

Montmorillonite (MMT) is a cheap, natural nano-mineral which improves the chemical, physical, mechanical, and thermal properties of many polymers as a result of its special layered structure and excellent distributed suspension, water-swelling, thixotropy, adhesion, ion exchange capacity, and organic adsorption behavior.[1–3] Accordingly, many technologies (*e.g.*, mechanical treatment, melt compounding, and *in situ* polymerization) have been developed to prepare such polymer-based clay nanocomposites.[4–17] An exfoliated dispersion of MMT is optimal for improving the properties of a polymer matrix. At present, the preparation of exfoliated nanocomposites generally follows a procedure in which MMT is first intercalated by an organic and cationic surfactant and then reactive monomers enter the open layers where they polymerize to form long-chain macromolecules that exfoliate the MMT into layers and sheets of nanoparticles. With this approach, however, it is difficult for MMT to undergo complete exfoliation, thereby setting a limit as to how far the properties of the polymer matrix can be improved. In addition, most organic surfactants that can be intercalated possess relatively low thermal degradation temperatures, meaning that would be a problem during melt compounding. As a result, the challenge remains to completely exfoliate MMT through a simple method to obtain polymer-based clay nanocomposites with relatively high thermal stability.

In this study, we used click chemistry to react singly and multiply functionalized azido-polyhedral oligomeric silsesquioxanes (N_3-POSS) with a propargyl-containing, long-alkyl-chain intercalator to prepare organic/inorganic hybrid surfactants for the exfoliation of MMT. POSS derivatives, unlike most silicones or fillers, are cage-like molecules presenting organic substituents on their outer surfaces, making them compatible or miscible with most polymers.[18] These functional groups can be designed to be either non-reactive (for polymer blending) or reactive (for copolymerization). For example, POSS derivatives presenting ammonium,[19] titanium-containing aminopropyl,[20] octakis(ammonium chloride),[21,22] alkyltrimethylammonium bromide,[23] aminopropylisooctyl polyhedral,[24–26] and imidazolium[27–29] units have been used to prepare intercalated clays and were then blended with reactive monomers or polymer matrices to form exfoliated polymer-based nanocomposites through melt compounding or *in situ* polymerization. In this study, we reacted *N*,*N*-dimethylstearylamine with propargyl bromide and then used the product to prepare intercalated MMT. Subsequently, we incorporated a POSS derivative functionalized with azido groups into the open layers of the intercalated MMT, where it reacted with the intercalator through click chemistry (Scheme 1) to form exfoliated MMT.

Experimental

Materials

MMT was purchased from Nanocor (USA); *N*,*N*-dimethylstearylamine and propargyl bromide were obtained from Tokyo Chemical Industry; *N*,*N*-dimethylformamide (DMF), sodium azide (NaN_3), ethanol, vinylbenzyl chloride, and *N*,*N*,*N*,*N*,*N*-pentamethyldiethylenetriamine (PMDETA) were purchased from Sigma–Aldrich. Copper (I) bromide (Sigma–Aldrich) (CuBr) was purified by washing with glacial AcOH overnight, followed by washing with absolute ethyl ether and then drying under vacuum. All solvents were distilled prior to use. The mono- and multi-functionalized azide-POSS derivatives were prepared according to previous reports.[30,31]

Preparation of intercalated-MMT (In-MMT)

A mixture of *N*,*N*-dimethylstearylamine (3.86 g, 130 mmol) and propargyl bromide (1.55 g, 130 mmol) in distilled water (100 mL) and EtOH (100 mL) was heated at 80 °C for 0.5 h with rapid stirring to form propargyldimethylstearylammonium bromide (PDS, Scheme S1, ESI†). MMT (10 g) was added to the solution, which was then stirred vigorously for 4 h. After cooling to room temperature, washing, filtering, drying, and grinding, In-MMT was obtained.

Department of Materials and Optoelectronic Science, National Sun Yat-Sen University, Kaohsiung, Taiwan E-mail: kuosw@faculty.nsysu.edu.tw
† Electronic supplementary information (ESI) available. See DOI: 10.1039/c2ra21917d

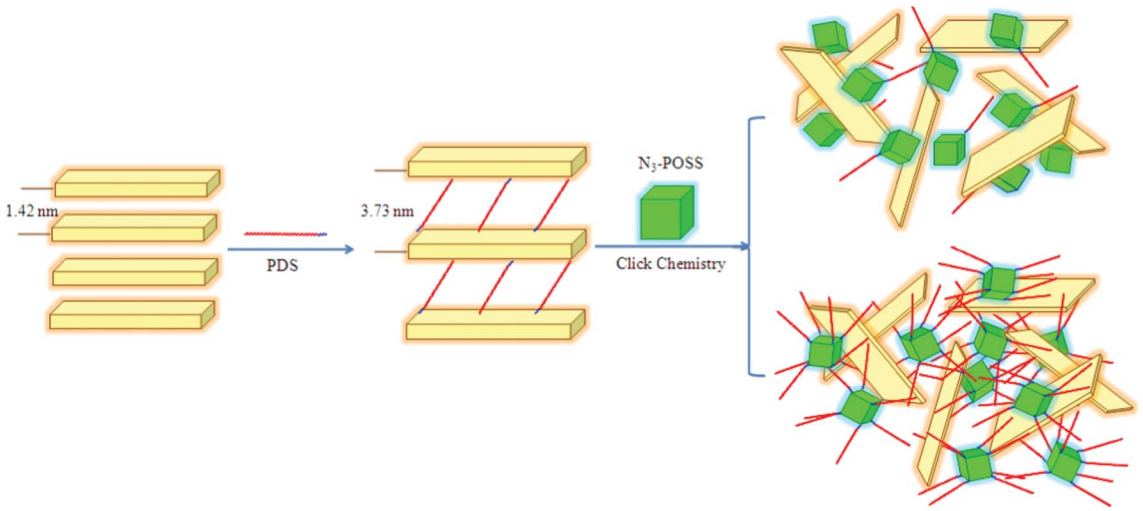

Scheme 1 Exfoliation of MMT through click reactions.

Preparation of exfoliated MMT (Ex-MMT) *via* click chemistry

Mono-functionalized azide POSS (N_3-POSS, 0.589 g, 0.500 mmol), In-MMT (0.521 g), and CuBr (0.0717 g, 0.500 mmol) were mixed together in the solid state under vacuum. After adding anhydrous DMF the mixture was stirred rapidly for 12 h under vacuum. Next, six freeze/thaw/pump cycles were performed, with the total time of freezing and pumping being 0.5 h and the time of the thaw, while strongly stirring, being 1 h in each cycle. At this point, PMDETA (0.100 mL, 0.500 mmol) was added and one freeze/thaw/pump cycle was performed again. After the final thaw to room temperature, the reaction mixture was stirred rapidly for 12 h under vacuum. After washing sequentially with anhydrous DMF and distilled water, filtering, drying, and grinding, Ex-MMT-A was obtained (Scheme S2(a), ESI†). Using the same procedure, Ex-MMT-B was also obtained (Scheme S2(b), ESI†) from multi-functionalized azide-POSS (1.15 g, 0.500 mmol) and In-MMT (0.521 g).

Characterization

Wide-angle X-ray diffraction (XRD) data were collected using a BL17A1 wiggler beam line of the National Synchrotron Radiation Research Center (NSRRC), Taiwan. A triangular bent Si (111) single crystal was employed to obtain a monochromated beam with a wavelength (λ) of 1.33001 Å. The value of $d_{(001)}$ was calculated using Bragg's law, $\lambda = 2d\sin\theta$, where λ is the wavelength of the X-rays, d is the distance between two MMT layers, and θ is the diffraction angle. Fourier transform infrared (FTIR) spectra of the sample pellets were recorded using a Bruker Tensor 27 FTIR spectrophotometer and the conventional KBr disk method; 32 scans were collected at a spectral resolution of 1 cm^{-1}; the pellets used in this study were sufficiently thin to obey the Beer–Lambert law. Transmission electron microscopy (TEM) images were recorded using a JEOL-2100 transmission electron microscope operated at an accelerating voltage of 200 kV. Ultrathin sections (thickness: *ca.* 70 nm) of the TEM samples were prepared using a Leica Ultracut UCT microtome equipped with a diamond knife; they were then placed onto Cu grids coated with carbon-supporting films. The thermal stabilities of the samples were measured using a TA Q-50 thermogravimetric analyzer operated under a pure N_2 atmosphere. The sample (*ca.* 7 mg) was placed in a Pt cell and heated at a rate of 20 °C min^{-1} from 30 to 800 °C under a N_2 flow rate of 60 mL min^{-1}.

Results and discussion

We used XRD to characterize the layered structures of the modified clays, because changes in diffraction angle can reveal variations in the

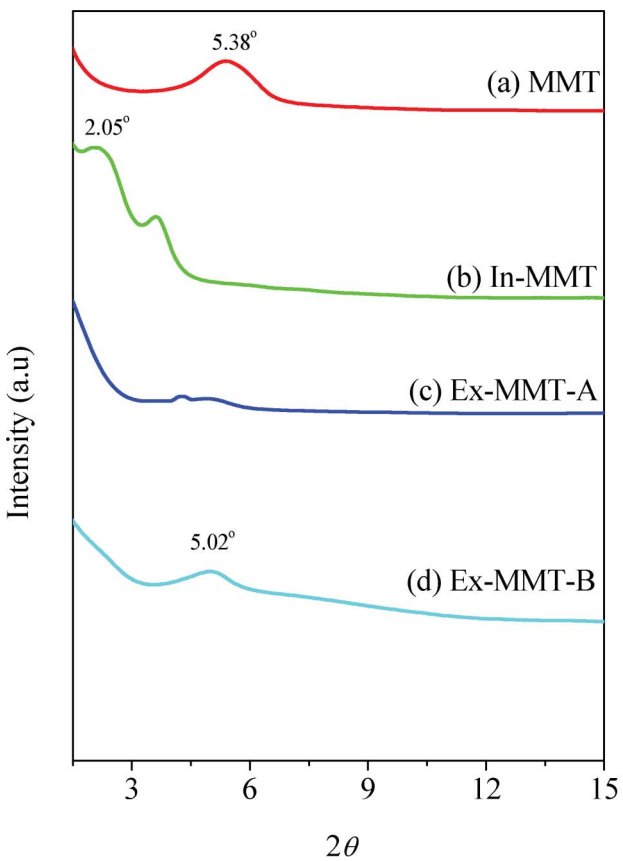

Fig. 1 XRD patterns of (a) pristine MMT, (b) In-MMT, (c) Ex-MMT-A, and (d) Ex-MMT-B.

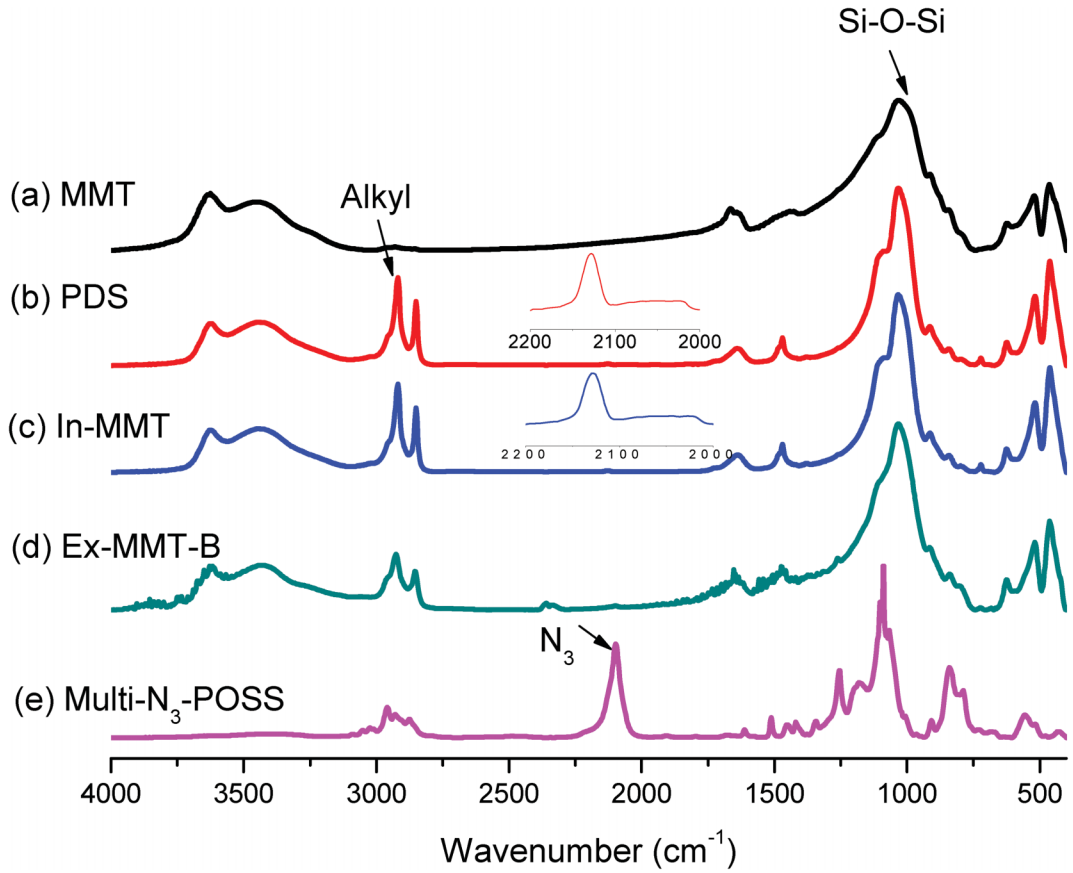

Fig. 2 FTIR spectra of (a) pristine MMT, (b) PDS, (c) In-MMT, (d) Ex-MMT-B, and (e) N_3-POSS.

gallery distance of the clay. Fig. 1 presents X-ray diffraction patterns of the pristine MMT, In-MMT, Ex-MMT-A, and Ex-MMT-B. The pattern of pristine MMT featured a peak at 5.38°, corresponding to a basal space of 1.42 nm; that of the PDS-modified MMT (In-MMT) exhibited a diffraction angle at 2.05°, corresponding to a basal space of 3.73 nm—much larger than that of pristine MMT. This observation implies that PDS had entered and opened the MMT layer to form a larger gallery distance, as confirmed through the signals of PDS in the FTIR spectrum of the intercalated clay sample (Fig. 2 and S1, ESI†).

The spectrum of pristine MMT featured a strong absorption peak at 1033 cm^{-1} for the Si–O–Si bond in the montmorillonite silicate; PDS provided absorption peaks at 2800–2950 cm^{-1}, representing its alkyl chain, and a very weak absorption at 2128 cm^{-1} for its acetylene unit. The absorption bands of In-MMT were a combination of those of pristine MMT and PDS, suggesting that the ordered layered structure remained. Fig. 3 displays the thermogravimetric analysis (TGA) traces of pristine MMT and PDS-treated MMT (In-MMT). The TGA trace of pristine MMT revealed only the loss of physically absorbed water and crystal water between layers and structural water in the layers; its total weight loss was only 6 wt% at temperatures up to 800 °C. In contrast, the organic surfactant (PDS)-intercalated MMT decomposed more readily, with the weight loss of In-MMT (*ca.* 40%) caused mainly by the pyrolysis of PDS at temperatures up to 600 °C, at which point the intercalator had pyrolyzed completely. TEM images of pristine MMT and In-MMT (Fig. 4) revealed that these two MMTs both possessed intercalated structures, consistent with the XRD analyses. To prepare exfoliated MMT, we performed Huisgen [2 + 3] cycloadditions (click reactions) between the propargyl units of intercalated PDS and singly or multiply azido-functionalized POSS nanoparticles. Based on the weight loss data from TGA analyses, we combined In-MMT aggregates containing the desired amounts of mono- or multi-functionalized azide-POSS derivatives with click chemistry to prepare exfoliated MMT.

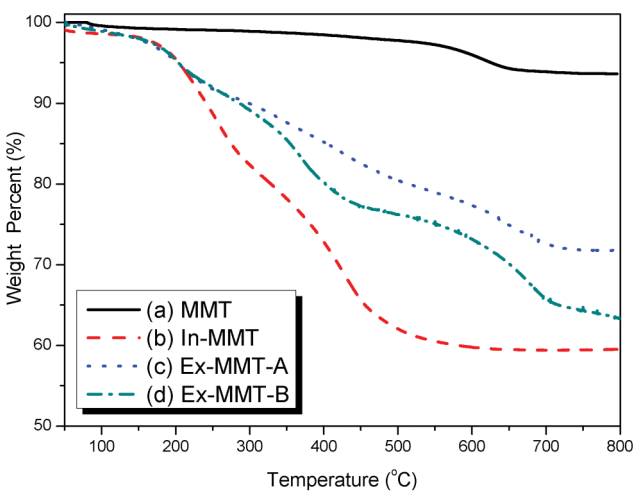

Fig. 3 TGA traces of (a) pristine MMT, (b) In-MMT, (c) Ex-MMT-A, and (d) Ex-MMT-B.

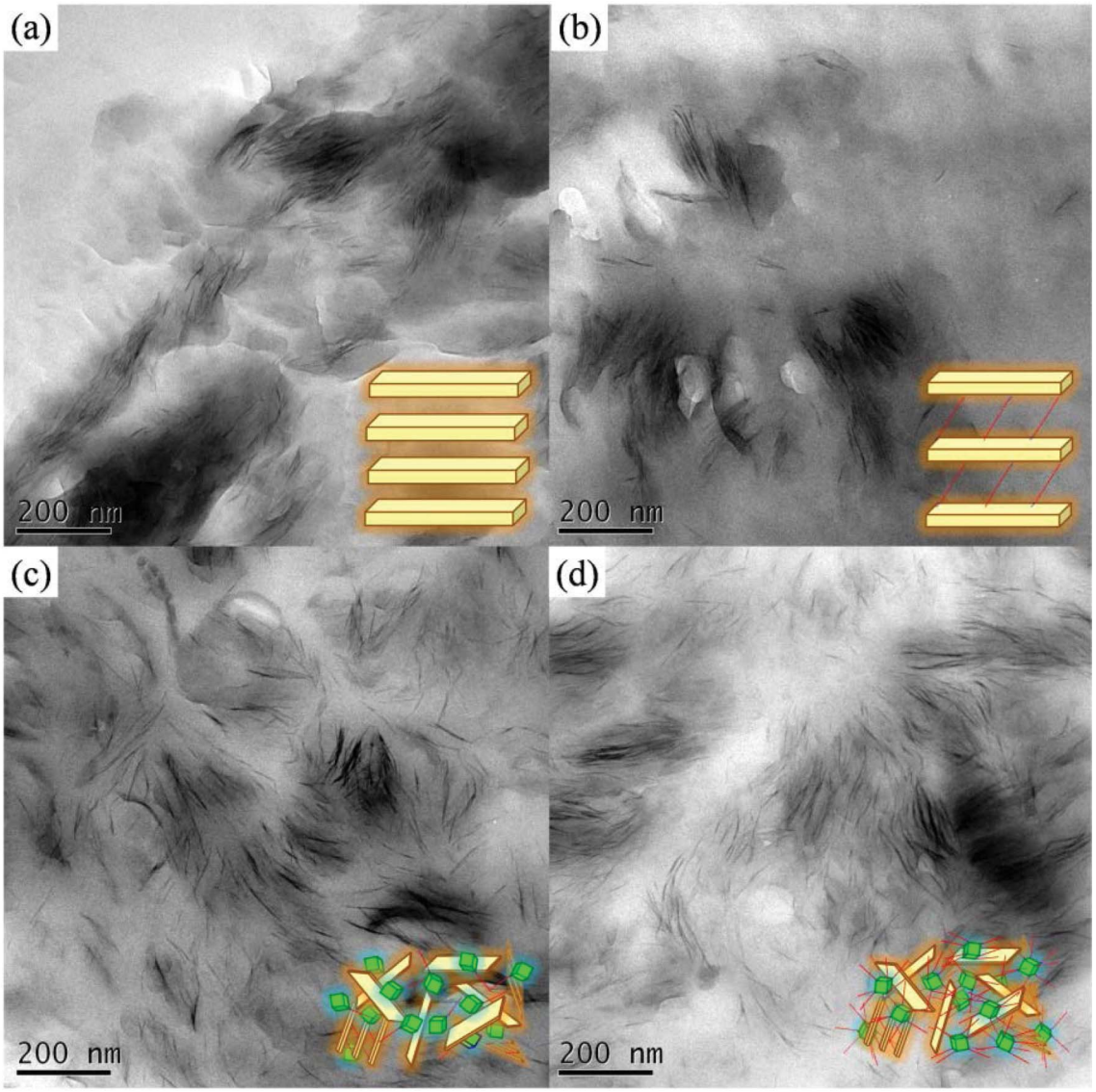

Fig. 4 TEM images (a) pristine MMT, (b) In-MMT, (c) Ex-MMT-A, and (d) Ex-MMT-B.

We used FTIR spectroscopy to determine the degrees of completeness of the click reactions by monitoring the signals for the azido and acetylene groups (Fig. 2 and S1, ESI†). The signal at 2100 cm^{-1} for the azido groups[32,33] in mono- and multi-functionalized azide-POSS (Fig. 2(e) and S1(c), ESI†) disappeared completely from the spectrum for the exfoliated MMT (Fig. 2(d) and S1(b), ESI†), while the characteristic Si–O–Si (siloxane) absorptions of POSS and MMT remained near 1100 cm^{-1},[34,35] indicating that all of the azido and acetylene functionalities had participated in the click reactions. For Ex-MMT-A and Ex-MMT-B, no diffraction peaks appeared within the range 0.5–5° in their XRD patterns (Fig. 1(c) and 1(d)), indicating that the MMT had exfoliated completely as a result of the click reactions (Scheme S2, ESI†). Diffraction peaks at 2θ values of approximately 5° embodied the crystal characteristics of the POSS moieties, confirming that the mono- and multi-functionalized azide-POSS derivatives had indeed entered between the layers of In-MMT and underwent subsequent click reactions with the acetylene groups of the PDS units, resulting in strong exfoliation of MMT. A similar phenomenon also appeared in intercalated nanocomposites of POSS-clay.[19,36] This showed a partial exfoliation with mostly intercalated states in Ex-MMT-A and Ex-MMT-B. Their TEM images (Fig. 4(c) and 4(d)) reveal that MMT had exfoliated into layers or sheets presenting POSS nanoparticles, which were dispersed randomly, in a disordered manner, with some layered structures. Most importantly, the char yields and decomposition temperatures of Ex-MMT-A and Ex-MMT-B were both higher than that of In-MMT. For example, In-MMT exhibited 10 wt% loss near 230 °C and a char yield of approximately 60 wt%; in contrast, Ex-MMT-A and Ex-MMT-B underwent 10 wt% losses near 330 and 290 °C, respectively, with char yields of approximately 72 and 64 wt%, respectively. The significant increases in decomposition temperature (*e.g.*, almost 100 °C higher for Ex-MMT-A than for In-MMT) arose because POSS is an inorganic material that delays the pyrolysis process; that is, the POSS-intercalated clays are thermally stable relative to the organic-intercalated clays. In addition, the char yield and decomposition temperature of Ex-MMT-A were higher than those of Ex-MMT-B because the weight percentage of the inorganic content of the mono-functionalized POSS was greater than

that of the multi-functionalized POSS. Notably, in previous studies using POSS derivatives as surfactants for the treatment of MMT,[19–29] only intercalated structures had been observed. In this present study, however, we obtained fully exfoliated structures when reacting a propargyl-functionalized intercalator with singly or multiply azido-functionalized POSS nanoparticles through click chemistry.

Conclusions

In this study we have combined inorganic POSS with click chemistry to fabricate exfoliated MMT. The POSS nanoparticles, which were functionalized with azido groups, entered into the layers of MMT that had been separated through intercalation of a propargyl derivative; subsequent click reactions exfoliated the MMT into layers or sheets of nanoparticles. We suspect that such exfoliated nano-MMT could be used directly for polymer blending or copolymerization to improve the properties of polymer-based clay nanocomposites. In future studies, we will use such products to improve the mechanical properties, especially the toughness and flexibility, of polymers.

Acknowledgements

This study was supported financially by the National Science Council, Taiwan, Republic of China, under contracts NSC 100-2221-E-110-029-MY3 and NSC 100-2628-E-110-001.

References

1 B. Q. Chen and J. R. G. Evans, *Soft Matter*, 2009, **5**, 3572–3584.
2 P. Kiliaris and C. D. Papaspyrides, *Prog. Polym. Sci.*, 2010, **35**, 902–958.
3 C. W. Chiu and J. J. Lin, *Prog. Polym. Sci.*, 2012, **37**, 406–444.
4 J. J. Lin, I. J. Cheng, R. C. Wang and R. J. Lee, *Macromolecules*, 2001, **34**, 8832–8834.
5 C. C. Chou, F. S. Shieu and J. J. Lin, *Macromolecules*, 2003, **36**, 2187–2189.
6 C. C. Chou, Y. C. Chang, M. L. Chiang and J. J. Lin, *Macromolecules*, 2004, **37**, 473–477.
7 C. C. Chu, M. L. Chiang, C. M. Tsai and J. J. Lin, *Macromolecules*, 2005, **38**, 6240–6243.
8 J. J. Lin, C. C. Chu, M. L. Chiang and W. C. Tsa, *J. Phys. Chem. B*, 2006, **110**, 18115–18120.
9 N. Sheibat-Othman, A. M. Cenacchi-Pereira, A. M. Dos Santos and E. Bourgeat-Lami, *J. Polym. Sci., Part A: Polym. Chem.*, 2011, **49**, 4771–4784.
10 R. F. A. Teixeira, H. S. McKenzie, A. A. Boyd and S. A. F. Bon, *Macromolecules*, 2011, **44**, 7415–7422.
11 F. Touchaleaume, J. Soulestin, M. Sclavons, J. Devaux, M. F. Lacrampe and P. Krawczak, *Polym. Degrad. Stab.*, 2011, **96**, 1890–1900.
12 C. L. Li, P. Choi and M. C. Williams, *Langmuir*, 2011, **26**, 4303–4310.
13 V. V. Ginzburg, J. D. Weinhold, P. K. Jog and R. Srivastava, *Macromolecules*, 2011, **42**, 9089–9095.
14 H. K. Fu, C. F. Huang, S. W. Kuo, H. C. Lin, D. R. Yei and F. C. Chang, *Macromol. Rapid Commun.*, 2008, **29**, 1216–1220.
15 W. Zhu, C. H. Lu, F. C. Chang and S. W. Kuo, *RSC Adv.*, 2012, **2**, 6295–6305.
16 C. Zhang, W. W. Tjiu, W. Fan, Z. Yang, S. Huang and T. Liu, *J. Mater. Chem.*, 2011, **21**, 18011–18017.
17 N. Greesh, R. Sanderson and P. C. Hartmann, *Polymer*, 2012, **53**, 708–718.
18 S. W. Kuo and F. C. Chang, *Prog. Polym. Sci.*, 2011, **36**, 1649–1696.
19 D. R. Yei, S. W. Kuo, Y. C. Su and F. C. Chang, *Polymer*, 2004, **45**, 2633–2640.
20 F. Carniato, C. Bisio, G. Gatti, E. Boccaleri, L. Bertinetti, S. Coluccia, O. Monticelli and L. Marchese, *Angew. Chem., Int. Ed.*, 2009, **48**, 6059–6061.
21 H. Z. Liu, W. Zhang and S. Zheng, *Polymer*, 2005, **46**, 157–165.
22 F. A. He and L. M. Zhang, *Nanotechnology*, 2006, **17**, 5941–5946.
23 L. Liu, L. Song, S. Zhang, H. Guo, Y. Hu and W. Fan, *Mater. Lett.*, 2006, **60**, 1823–1827.
24 C. Wan, F. Zhao, X. Bao, B. Kandasubramanian and M. Duggan, *J. Phys. Chem. B*, 2008, **112**, 11915–11922.
25 J. H. Lee and Y. G. Jeong, *Fibers Polym.*, 2011, **12**, 180–189.
26 A. McLauchlin, X. Bao and F. Zhao, *Appl. Clay Sci.*, 2011, **53**, 749–753.
27 D. M. Fox, P. H. Maupin, R. H. Harris, J. W. Gilman, D. V. Eldred, D. Katsoulis, P. C. Truolve and H. C. De, *Langmuir*, 2007, **23**, 7707–7714.
28 D. M. Fox, R. H. Harris, S. Bellayer, J. W. Gilman, M. Y. Gelfer, B. S. Hsiao, P. H. Maupin, P. C. Trulove and H. C. Long, *Polymer*, 2011, **52**, 5335–5343.
29 J. K. H. Teo, C. L. Toh and X. Lu, *Polymer*, 2011, **52**, 1975–1982.
30 K. W. Huang and S. W. Kuo, *Macromol. Chem. Phys.*, 2010, **211**, 2301–2311.
31 Y. C. Lin and S. W. Kuo, *J. Polym. Sci., Part A: Polym. Chem.*, 2011, **49**, 2127–2137.
32 D. J. Clarke, J. G. Matisons, G. P. Simon, M. Samoc and A. Samoc, *Appl. Organomet. Chem.*, 2010, **24**, 184–188.
33 K. W. Huang and S. W. Kuo, *Macromol. Chem. Phys.*, 2012, **213**, 1509–1519.
34 B. P. Nair and C. Pavithran, *Langmuir*, 2010, **26**, 730–735.
35 W. J. Zhu, C. H. Lu, F. C. Chang and S. W. Kuo, *RSC Adv.*, 2012, **2**, 6295–6305.
36 H. K. Fu, S. W. Kuo, D. R. Yeh and F. C. Chang, *J. Nanomater.*, 2008, 739613.